Pakistan Veterinary Journal

ISSN: 0253-8318 (PRINT), 2074-7764 (ONLINE)
DOI: 10.29261/pakvetj/2026.247

RESEARCH ARTICLE

Characterization of Pre-Theca Cells in Chicken Embryonic Ovaries for Productivity

Lintian Yu[1*], Ali Raza Jahejo[2*], Xiaoyan Xiong[3], and Mikhlid H. Almutairi[4]

[1]Ganzhou Polytechnic, Ganzhou, Jiangxi province, 341000, China; [2]Guangxi Key Laboratory of Animal Breeding, Disease Control and Prevention, College of Animal Science and Technology, Guangxi University, Nanning, 530004 China; [3]Infectious Disease Epidemiology Group, Wageningen University, PO Box 338, 6700 AH Wageningen, The Netherlands; [4]Department of Zoology, College of Science, King Saud University, P.O. Box 2455, Riyadh 11451, Saudi Arabia
*Corresponding author: 2018401009@st.gxu.edu.cn (LY), arjahejo@gmail.com (ARJ)

ARTICLE HISTORY (26-1137)

Received: September 19, 2026
Revised: October 22, 2026
Accepted: October 25, 2026
Published online: October 28, 2026

Key words:
Ovarian reserve
Poultry
Pre-theca cells
Productivity
Steroidogenesis

ABSTRACT

In poultry, size and quality of the initial pool of primordial follicles, known as ovarian reserve, play a key role in female reproductive lifespan and productivity. The molecular and cellular characterization of the pre-theca cells that drive steroid hormone synthesis and assembly of ovarian reserves in chickens are not well known. A multi-omics approach was used in this study, which analyzed gonadal data of chickens, humans and mice to find and characterize pre-theca cells. The fluorescence in situ hybridization (FISH) was used to verify pre-theca cells. Chicken pre-theca cells were found as early as in the ovary prior to primordial follicle development in single cell mRNA sequencing (scRNA_seq) data analysis. A probe of the *CYP11A1* gene verified the presence of pre-theca cells during the formation and activation of primordial follicles. Further, 10 candidate genes that can distinguish pre-theca cells in chicken were identified by the scRNA-seq analysis. The pseudo-time analysis showed that the trajectory of chicken pre-theca cells is linear. On the basis of the data of differential expression, the genes that are significantly up-expressed in female gonads were *CYP17A1*, *TXN*, *SPON1*, *BASP*1 and *APOA1* during chicken's sex determination. Lipid metabolism, steroid synthesis and steroid hormone synthesis were significantly enriched in chicken pre-theca cells. These results indicate that pre-theca cells establish an early, specialized steroidogenic microenvironment, and provide a molecular foundation for understanding early ovarian niche formation and reproductive potential in poultry.

To Cite This Article: Yu L, Jahejo AR, Xiong X, and Almutairi MH, 2026. Characterization of pre-theca cells in chicken embryonic ovaries for productivity. Pak Vet J, 46(10): 2420-2432. http://dx.doi.org/10.29261/pakvetj/2026.247

INTRODUCTION

In poultry, the size and quality of the initial primordial follicles pool (ovarian reserve) is of paramount importance in determining the female's reproductive longevity and productivity. Pre-theca cells are the precursors of theca cells and are of critical importance in the ovary at the preantral stage in vertebrates. In the endocrine system of the ovary, it functions to supply the structural, metabolic and steroidogenic support required for normal ovarian and follicular development (Erickson *et al.*, 1985 ;Hirshfield, 1991 ;Edson *et al.*, 2009). In humans, primordial follicles are formed at 20 weeks after conception (wpc), activated primordial follicles at 23-26 wpc, and a few preantral and antral follicles develop by 37-40 wpc (Ford *et al.*, 2020). In mice, however, primordial follicles are established postnatally, and secondary follicles are normally present at about 7 days after birth (Kerr *et al.*, 2006 ;Lo *et al.*, 2019). The expression of *CYP11A1*, *CYP17A1*, *HSD3B1*, and *STAR* can be used to identify theca cells in these secondary and antral follicles (Li *et al.*, 2020 ;Yuan *et al.*, 2022). Interestingly, these canonical marker genes are not expressed in the mammalian embryonic ovary before the appearance of secondary follicles (Lenz *et al.*, 2004 ;Schwartz and Roy, 2000), suggesting that mammalian pre-theca cells do not express these markers before secondary follicles.

Theca cells are located in the outermost layer of antral and hierarchical follicles of the chicken ovary and are specifically characterized by the expression of *CYP11A1*, *CYP17A1*, and *HSD3B1* (Lu *et al.*, 2024). Unlike mammals, these canonical theca cell marker genes are

expressed early in the avian embryonic gonad, including that of chickens, ducks and zebra finches (Yang *et al.*, 2022 ;Jung *et al.*, 2021). The time of gonadal sex differentiation in chicken has been suggested to be between E4.5 and E6.5 (Nakata *et al.*, 2013 ;Smith and Sinclair, 2004), with mRNA transcriptomic analyses possibility of *CYP19A1* and *CYP11A1* being involved in this process (Ayers *et al.*, 2015). Moreover, day 5.5-19 incubated embryos showed that expression for *FSHR*, *CYP17A1*, *CYP11A1* and *HSD3B1* are expressed at a significantly higher level at later stages of the embryonic ovarian development (Carré *et al.*, 2011). CYP11A1, CYP17A1 and HSD3B1 are all critical genes that regulate the process of steroidogenesis (LaVoie and King, 2009); in particular, CYP11A1 converts cholesterol to pregnenolone, and CYP17A1 is crucial for the steroid hormone biosynthesis process. Our recent findings, that the pharmacological blockade of the steroid hormone synthesis pathway was sufficient to completely prevent primordial follicles to develop, indicating that the cells that synthesize these hormones are key to the establishment of the ovarian reserve. (Yu *et al.*, 2024). Moreover, *HSD3B1* is involved as an important regulator, transforming pregnenolone to progesterone and dehydroepiandrosterone to androstenedione. (Mourikes *et al.*, 2023). Thus, the early appearance of pre-theca cells is likely to play an important role in the gonadal development and sex differentiation of the female chicken.

The molecular characterization and the functions of chicken pre-theca cells during the formation of the ovarian reserve are still not known. Thus, in the present study, we aimed to identify chicken pre-theca cells and explore their molecular characteristics, and also to understand the function of the primordial follicle pool through a multi-omics approach.

In this study, 'pre-theca cells' refers to an early steroidogenic stromal population present before the emergence of hierarchical follicles, distinct from the mature theca cells of antral and hierarchical follicles. The aim of this study is to broaden the existing knowledge on the development of chicken ovaries and to further lay the foundation for future research on maximizing the reproductive health and fertility in poultry. Furthermore, this study provides a foundation for future research into the mechanisms of avian gonadal sex determination.

MATERIALS AND METHODS

Sampling: A total of 40 Guangxi Ma chickens (Females) were obtained from Guangxi Fufeng Agriculture and Animal Husbandry Co., Ltd. and fed and watered *ad-libitum*. To assess the expression of pre-theca markers, left ovaries were collected from chickens at four post-hatch time points: 2, 5.5, 10.5 and 15 days post hatching (dph). Furthermore, these samples were used for Hematoxylin, and Eosin (H&E) staining and Fluorescence in situ hybridization (FISH) experiments.

Integration of dataset: Chicken post-hatch ovarian scRNA-seq data (2, 5.5, and 10.5 dph; 31,808 total cells post-QC: 12,269 at 2 dph; 9,896 at 5.5 dph; and 9,643 at 10.5 dph) were obtained from our previously published dataset (PRJNA1060270; (Yu *et al.*, 2024)). Chicken embryonic gonadal scRNA-seq data (E4.5, E6.5, E8.5, and E10.5; pooled embryonic gonads per stage) were obtained from PRJNA600155 (Estermann et al., 2020). Sex-reversal transcriptomic profiles of E10 gonads (n=3 biological replicates each for FE10, ME10, and RE10) were obtained from PRJNA867032. E6.5 embryonic gonadal proteomics data (n=3 biological replicates per group: FnL, FnR, MnL, MnR) were retrieved from PXD035373. For cross-species comparisons, mouse ovarian scRNA-seq (E11.5–P5; n=2–3 replicates per stage) was obtained from PRJNA971592 and human embryonic gonadal scRNA-seq (9, 14 and 21 wpc; n=1–2 donors per stage) was acquired from ArrayExpress (E-MTAB-10551). All single-cell datasets were filtered using uniform QC criteria (cells with >300 detected genes and <15% mitochondrial reads), normalized with a scale factor of 104 and clustered using the top 30 principal components at a resolution of 0.4. Differential expression was determined using a two-sided Wilcoxon rank-sum test (adjusted $P<0.01$, $|avg_log2\ FC|>1$|avg_log 2 FC|>1).

Histological analysis: A total (n=6, left ovaries) of chicken was collected for morphological evaluation. For 24 h, it was fixed with Bouin's fixative solution (PH0976, Phygene, China), washed with phosphate-buffered saline (PBS) and stored in 70% ethanol at 4°C. It was then subjected to a graded series of dehydration (75 to 100% ethanol), followed by xylene clearing, and then embedded in paraffin and cut into 5μM sections with an automatic rotary microtome (RM2255, Leica, Germany). Five sections were taken for each specimen (inter-slice distance of 50μM) and they were stained using a standard H&E staining kit (G1120, Solarbio, Beijing, China). Images of the sections were acquired using an EVOS™ M5000 Imaging System (Invitrogen, Thermo Fisher Scientific, USA) and total of 6 fields were taken from each section for image analysis.

Fluorescence in situ hybridization (FISH): Chicken ovaries (n=3 per group) were washed with PBS containing diethylpyrocarbonate (DEPC) and fixed in 4% paraformaldehyde (containing 1/1000 DEPC). Paraffin sections (8μM thickness) were prepared and mounted on Polysine™ microscopy slides. Sections were dewaxed and treated with freshly diluted pepsin in 3% citric acid at 37°C for 20 minutes to facilitate mRNA accessibility. Following washes with 0.5M PBS and distilled water, mRNA hybridization was performed using a specific *CYP11A1* probe (F32947, Alexa Fluor™ 488, Thermo Fisher Scientific) according to the manufacturer's protocol.

Single-cell transcriptomic analysis of ovarian cell populations: The GRCg6a reference genome and corresponding annotations were obtained from the Ensembl genome browser and processed using Cell Ranger (v6.0.0) following the standard 10x Genomics pipeline. Subsequent analyses were conducted in R (v4.3.1) using the Seurat package (v4.3.0.1). Quality control was performed by excluding cells with fewer than 300 detected genes or a mitochondrial gene percentage exceeding 15%. Data were normalized using the global-scaling method (scale factor = 10^4) and log-transformed. The top 2,000

highly variable genes were identified using the "vst" selection method. Dimensionality reduction was performed via Principal Component Analysis (PCA) on the top 30 principal components, and cells were clustered at a resolution of 0.4 and visualized using Uniform Manifold Approximation and Projection (UMAP).

Analysis of pre-theca cell maturation and intercellular signaling: The differentiation trajectory of pre-theca cells was analyzed using Monocle3 (v1.3.1) employing the DDR-tree algorithm. Branch expression analysis modeling (BEAM) was used to identify genes driving branch destiny. To evaluate the developmental potential and stemness of pre-theca cell subpopulations, CytoTRACE (v1.0.0) analysis was performed. Intercellular communication networks were constructed using the Cell Chat package (v1.5.0) based on ligand-receptor expression patterns to identify autocrine and paracrine signaling between cell clusters.

Proteomics and differential expression analysis: For proteomic identification, raw MS files were processed using the MaxQuant (v2.0.3.0) search engine against the chicken Ensembl reference database (GRCg6a) using label-free quantification (LFQ) with a false discovery rate (FDR) <0.01 for both proteins and peptides, requiring a minimum of two unique peptides. Differentially abundant proteins between female and male embryonic gonads were identified using a two-tailed Student's *t*-test with Benjamini–Hochberg FDR correction, applying significance cutoffs of adjusted P<0.05 and $|\log_2 FC| > 1.5$. Single-cell differentially expressed genes (DEGs) across clusters and developmental stages were identified using the FindMarkers function in Seurat (v4.3.0.1) via a two-sided Wilcoxon rank-sum test with Bonferroni correction (parameters: min.pct = 0.25, logfc.threshold = 0.25). Genes with an adjusted P<0.01 and $avg_log_2FC > 1.0$ were defined as significantly upregulated, and those with adjusted P<0.01 and $avg_log_2FC < -1.0$ as downregulated. For bulk transcriptomic analysis of sex-reversed gonads, differential expression was analyzed using DESeq2 (v1.40.2), with significance established at Benjamini–Hochberg adjusted P<0.05 and $|\log_2 FC| > 1.0$. Gene Ontology (GO) and KEGG functional enrichment analyses were performed using clusterProfiler (v4.10.0), with significance defined at an adjusted P<0.05.

RESULTS

Identification of pre-theca cells as components of the ovarian reserve: scRNA-seq data from chicken embryonic gonads (E4.5, E6.5, E8.5 and E10.5) and post-hatch ovaries (2, 5.5 and 10.5 dph) were integrated and analyzed for the Identification of pre-theca cells as components of the ovarian reserve. Unsupervised clustering identified 17 distinct cell populations (Fig. 1A, B). Cluster 10, characterized by the expression of *DDX4* and *DAZL*, was annotated as germ cells, while Cluster 1, expressing *CYP19A1*, was identified as granulosa cells. Cluster 4 expressed *CYP11A1*, *CYP17A1*, *STAR*, *HSD3B1*, *NR5A1* and *LHCGR*, and was distinct from the granulosa (*CYP19A1*) and germ cell (*DDX4*, *DAZL*) clusters. Together with its outer-layer localization in our previous spatial transcriptomic data (Yu *et al.*, 2024), this population was designated as pre-theca cells. Analysis of cell proportions suggested that Cluster 4 was present across all sampled developmental stages (Fig. 5A). Further differential expression analysis using FindMarkers, *CYP17A1*, *CYP11A1*, *STAR*, *TPM2*, *HSPE1*, *HSD3B1*, *SMAD7*, *NR5A1*, *SMAD5* and *LHCGR* were highly expressed in Cluster 4, which was identified as the major steroidogenic population essential for early ovarian development (Fig. 1C). We examined whether this early emergence of pre-theca cells is a conserved feature in vertebrate species by comparing our data with scRNA-seq data from human and mouse embryonic gonads. In human female embryonic gonads (9, 14 and 21 wpc) 23 cell clusters were identified (Fig. 1D). In the human embryonic ovary, expression of the canonical pretheca markers *CYP11A1*, *CYP17A1* and STAR were not detected, although feature plots suggest expression of germ cell markers (*DDX4*, *DAZL*) and granulosa cell markers (*CYP19A1*) (Fig. 1E). Likewise, integrated analysis of female mouse ovaries (from E11 to P5) revealed 28 cell clusters (Fig. 1F), showing that germ cells express *DDX4* and *DAZL* and granulosa cells express *Kitl* (Fig. 1G). The markers *CYP11A1*, *CYP17A1* and Star were not found in the mouse scRNA-seq data set.

The comparative results show that the molecular mechanisms behind ovarian reserve differentiation are quite different in chickens compared to humans or mice, and that the differentiation occurs earlier in chickens.

Establishment of pre-theca cells prior to the primordial follicle pool: To validate the spatiotemporal differentiation of pre-theca cells, chicken left ovary tissues were analyzed via H&E staining across multiple developmental time points (Fig. 2A). On histological examination primordial follicles were not present at 2 dph but were present from 5.5 dph. At 10.5 dph, a subpopulation of primordial follicles showed typical activation morphology with pre-granulosa cells changing from a flattened strip-like shape to more rounded, cuboidal shape. Primary follicles appeared by 15 dph consisting of an oocyte surrounded by several layers of pre-granulosa cells with an outermost layer of pre-theca cells. These pre-theca cells had considerably elongated (spindle-shaped) nuclei instead of the standard sphericity.

A probe for the mRNA of *CYP11A1* was used for fluorescence in situ hybridization (FISH) to identify the molecular onset of theca cell differentiation. The results showed expression of *CYP11A1* was found in the ovarian tissue as early as 2 dph and continued to be expressed at 5.5, 10.5 and 15 dph (Fig. 2B). In tissues from 10.5 and 15 dph, the signals of *CYP11A1* were highly localized to pre-theca cells of the outermost layer of primordial and primary follicles.

All these results together give important indications that molecular differentiation of pre-theca cells (as evidenced by *CYP11A1* expression) takes place before the morphological signs of primordial follicles. This suggests that the pre-theca cell population is present before the primordial follicle pool is formed. This demonstrates that pre-theca cells undergo molecular and morphological differentiation prior to the assembly of the primordial follicle pool, suggesting they establish an early structural and steroidogenic niche that accompanies the formation of the ovarian reserve.

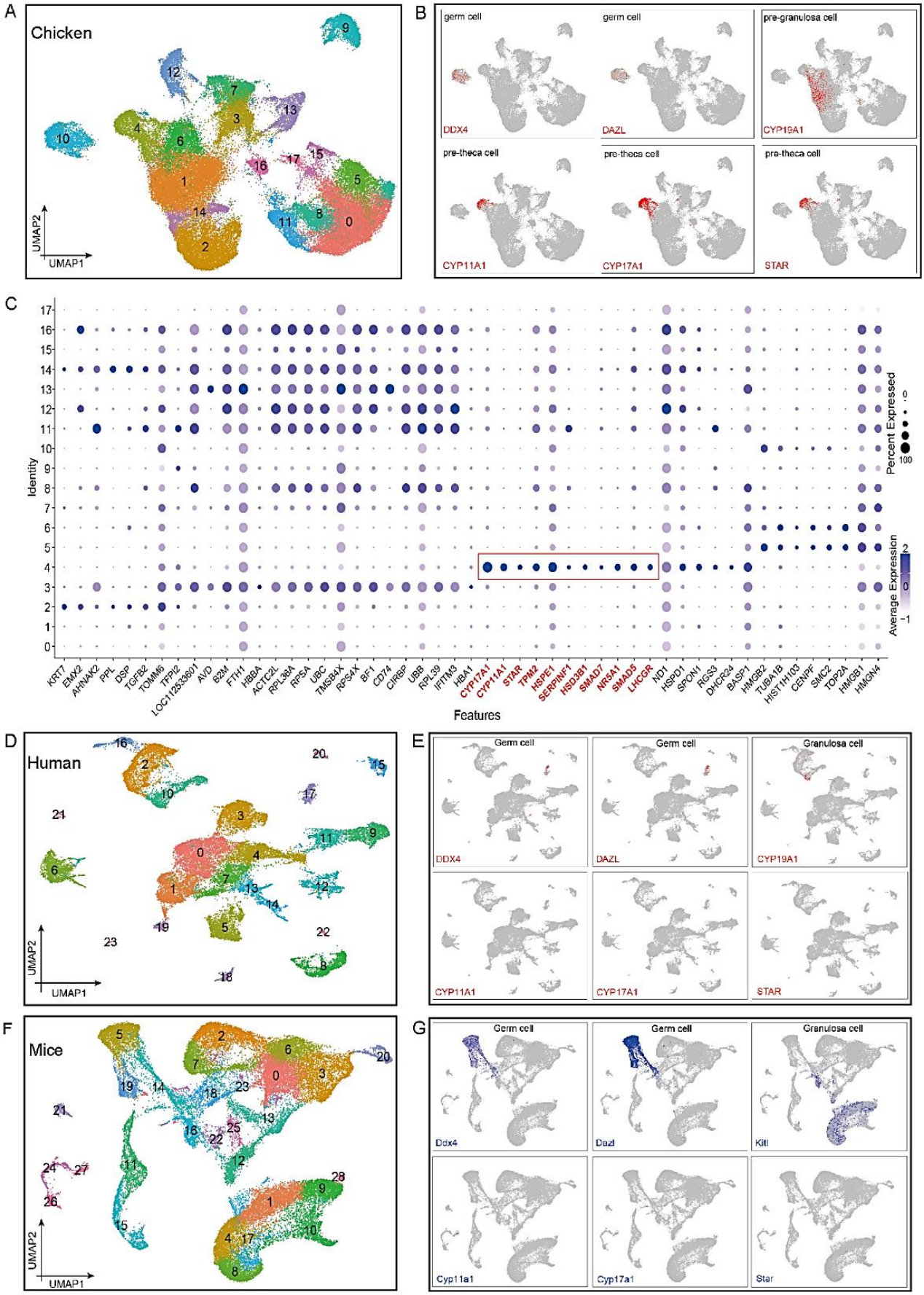


Fig. 1: Comparative analysis of early pre-theca cell emergence and its conservation across species: (A) UMAP visualization of cell clusters in chicken ovarian tissues. (B) Feature plots showing the expression of canonical marker genes in chickens. (C) Dot plot representing the expression levels and percentage of cells expressing marker genes across the identified clusters. (D) UMAP visualization of cell clusters in human female embryonic gonads. (E) Feature plots of corresponding markers in human embryonic ovaries. (F) UMAP visualization of cell clusters in neonatal female mouse ovaries. (G) Feature plots of corresponding markers in mouse ovaries.

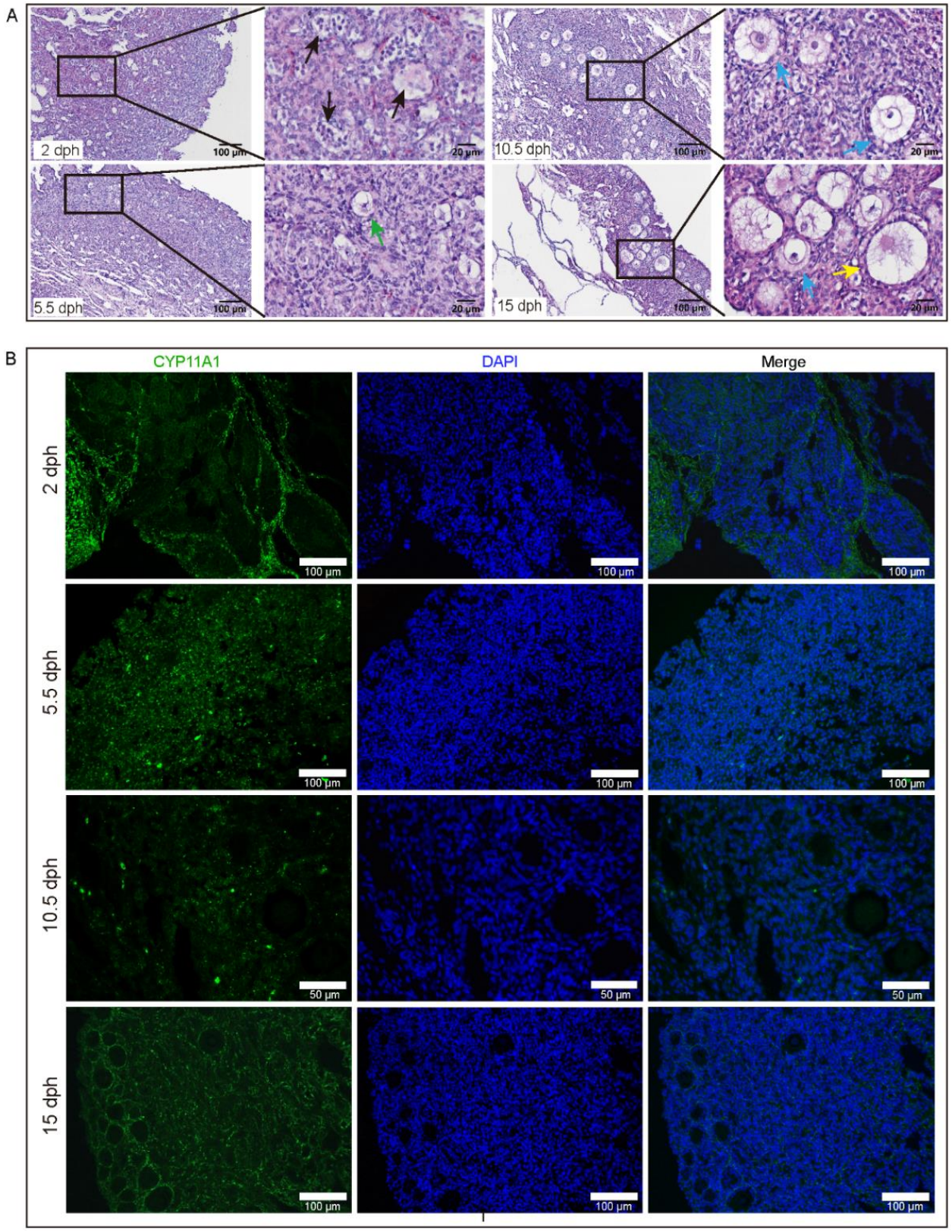


Fig. 2: Temporal establishment of pre-theca cells prior to the formation of the primordial follicle pool: (A) Representative H&E stained sections of chicken ovarian tissues at 2, 5.5, 10.5, and 15 dph. Black and green arrows indicate germ cell cysts and primordial follicles, respectively; blue and yellow arrows indicate pre-theca cells and pre-granulosa cells, respectively. (B) Fluorescence in situ hybridization (FISH) analysis for *CYP11A1* mRNA expression in chicken ovaries across the same time points. Scale bar = 100μM.

Developmental trajectory of pre-theca cells: Transcriptomes of pre-theca cells at different stages of maturation were compared using cytoTRACE and Monocle3 to gain a deeper understanding of the maturation process.

The analysis showed that the pre-theca population is divided into three subpopulations that have different expression profiles of canonical markers (Fig. 3A). The highest expression of steroidogenic genes (*CYP11A1*, *CYP17A1*, *HSD3B1*, and *NR5A1*) was seen in subgroup 0,

while the proliferation marker TOP2A was generally expressed in subgroup 2 (Fig. 3B). CytoTRACE analysis was used to predict cell stemness of these clusters to establish their developmental hierarchy. The highest stemness score was seen for the subgroup 2 cells, indicating that they are the most undifferentiated and earliest stage of pre-theca cell development (Fig. 3C).

Subsequently, pseudotime analysis was applied to infer a putative developmental trajectory among the three subpopulations (Fig. 3D). This computationally modeled trajectory predicts a progression from subgroup 2 (characterized by higher stemness and TOP2A expression) toward subgroup 0 (the mature steroidogenic state). The dynamics changes in the gene expression along this trajectory were further examined to identify maturation markers (Fig. 3E). All the canonical steroidogenic markers such as CYP11A1, CYP17A1, STAR, HSD3B1, SMAD5 and SMAD7 showed a consistent trend of increasing in the pseudotime axis as cells progressed. Notably, NR5A1 expression was only observed at the terminal stage of the trajectory, whereas NR5A2 was never detected in any of the pre-theca cell subgroups. All these results indicate that there is a linear maturation process in which the pre-theca cells acquire a steroidogenic function that is necessary to support the growth of the ovarian reserve.

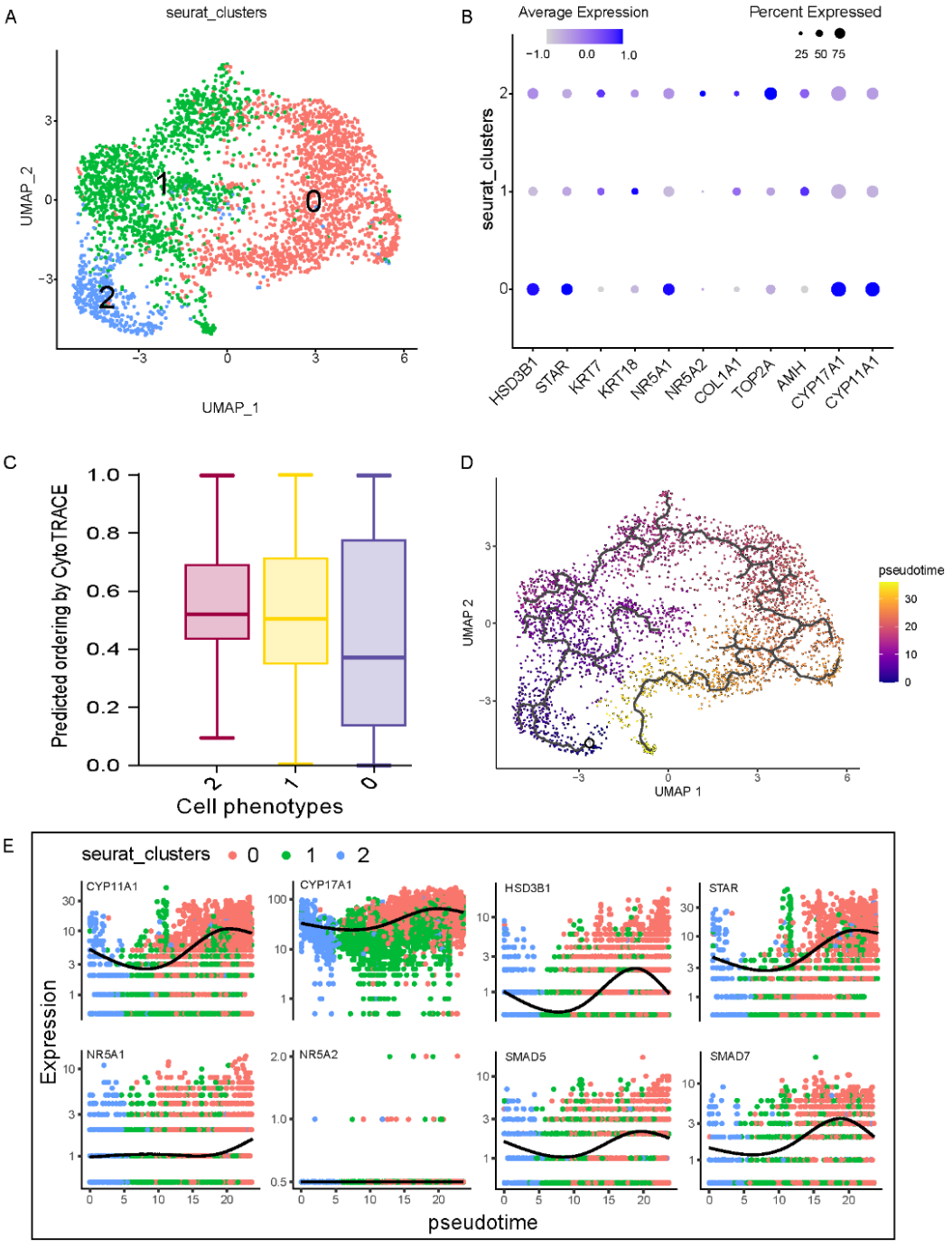


Fig. 3: Maturation trajectory and acquisition of steroidogenic identity in chicken pre-theca cells: (A) UMAP visualization of the three pre-theca cell subpopulations. (B) Dot plot showing the differential expression of maturation and proliferation markers across pre-theca subgroups. (C) Predicted stemness scores for pre-theca cell subpopulations as determined by cytoTRACE. (D) Pseudotime developmental trajectory reconstructed via Monocle3. (E) Expression dynamics of steroidogenic marker genes along the pre-theca cell developmental trajectory.

Pre-theca cell markers and ovarian development: To investigate the role of pre-theca cells in sex differentiation and ovarian development, we first studying the proteomic changes of the embryonic gonads from E6.5 embryos. Based on the Principal Component Analysis (PCA), the samples from the left and right gonads of female (FnL and FnR) were grouped together, whereas the male gonadal samples (MnL and MnR) were clearly separated (Fig. 4A), suggesting that the proteomic profiles were sufficiently distinct for further analysis. The results of hierarchical clustering and heatmap analysis also revealed that proteins CYP11A1, CYP17A1, NR5A1, STAR, TPM2, DHCR24, and CYP19A1 were only highly enriched in female embryonic gonads, while proteins SOX9, AMH, and DMRT1 were highly expressed in male tissues (Fig. 4B). To compare these female-specific profiles, we analyzed scRNA-seq data from male chicken gonads (E4.5–E10.5) that revealed 18 distinct cell clusters (Fig. 5B). Among these, the Cluster 0 cells had high expression of *AMH*, *SOX9*, CYP11A1 and *DMRT1*, indicating that this cluster was enriched with Sertoli cells, the male counterparts of the supporting cells of the ovary (Fig. 5C).

Finally, we utilized mRNA transcriptomic data from E10 chicken embryonic gonads to evaluate pre-theca cell expression profiling in a sex-reversal model. 3D-PCA analysis revealed distinct clustering for the male, female, and sex-reversed groups, indicating a significant divergence in their transcriptomic signatures (Fig. 4C). A heatmap of representative genes after $\log_2$ transformation showed that 595 genes were significantly upregulated in the female group compared to the sex-reversed group, including *CYP19A1, IGF1, TGIF1, CALB1, GREB1, TPM2, FSHR* and *FOXL2* (Fig. 4D). Notably, the canonical pre-theca marker genes—*CYP11A1, CYP17A1, STAR, NR5A1* and *LHCGR*—showed higher expression in the female group, although their $\log_2$ fold-change values were below 1.5. Conversely, the male-specific markers *AMH* and *SOX9* were significantly upregulated in both the male and sex-reversed groups. These results indicate that the expression of pre-theca cell markers is strictly tied to the female developmental program and is suppressed during sex reversal, strongly suggesting that the differentiation of pre-theca cells is an essential requirement for the female-specific establishment of the ovarian reserve.

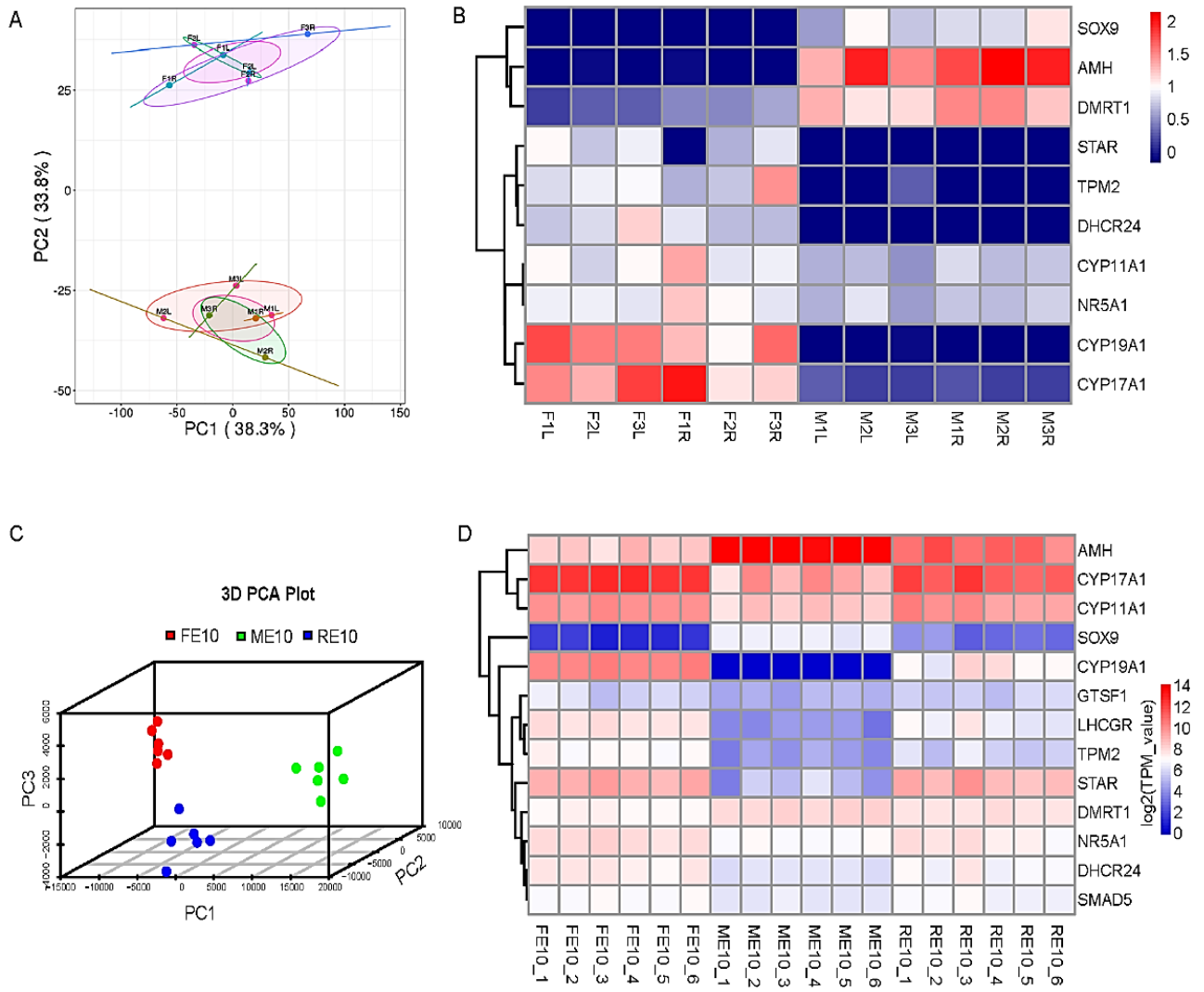


Fig. 4: Proteomic and transcriptomic markers of female-specific gonadal development and reproductive health: (A) PCA plot of embryonic gonadal proteomic profiles at E6.5. (B) Heatmap of differentially expressed proteins in female versus male embryonic gonads at E6.5. (C) 3D-PCA plot illustrating the separation of female (FE10), male (ME10), and sex-reversed (RE10) embryonic gonads at E10. (D) Heatmap showing the expression of representative genes in FE10, ME10, and RE10 groups after $\log_2$ transformation.

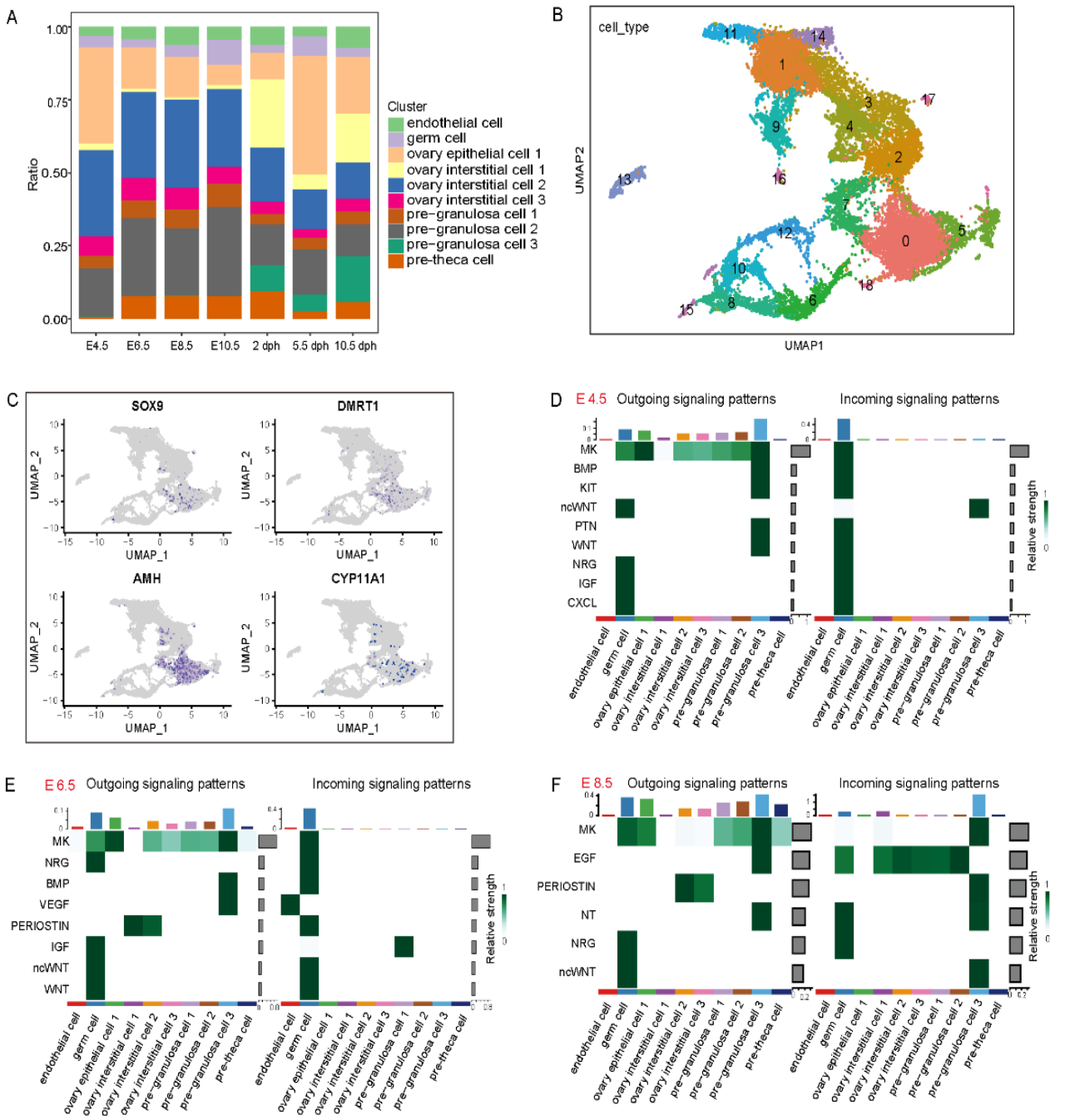


Fig. 5: Cellular composition of male gonads and the role of pre-theca cells as influencers of the ovarian niche: (A) Proportion of ovarian cell types across the sampled developmental stages. (B) UMAP visualization of cell clusters identified in male chicken gonads. (C) Feature plots showing the expression of *SOX9, DMRT1, AMH,* and *CYP11A1* in male gonadal clusters. (D–F) Heatmaps of outgoing and incoming signaling patterns in female chicken gonads at E4.5 (D), E6.5 (E), and E8.5 (F).

Metabolic pathway and regulatory genes governing ovarian reserve: To elucidate the molecular mechanisms by which pre-theca cells contribute to gonadal development, we performed a comparative transcriptomic analysis between E4.5 and E6.5 embryonic gonads. We identified 129 differentially expressed genes (DEGs) within the pre-theca cell population (Table 1). Among these, five genes—*CYP17A1, TXN, SPON1, BASP1,* and *APOA1*—exhibited significant upregulation at E6.5 compared to E4.5. Gene Ontology (GO) enrichment analysis revealed that these candidate genes were primarily associated with cell adhesion, lipid metabolism, and lipid biosynthesis pathways (Fig. 6A), suggesting a shift toward a specialized metabolic state necessary to fuel the establishment of the ovarian reserve during the critical window of development.

To gain more insight into the protein-protein interaction (PPI) network of these DEGs, we selected 12 core proteins with high connectivity. In this network, ribosomal proteins such as RPS19, RPS21, RPS25, RPS26, RPS27 and RPL14 were among the most abundant proteins in the pre-theca cell network, suggesting that it was a network of proteins involved in high levels of protein synthesis and metabolic activity in pre-theca cell maturation (Fig. 6B). Notably, a significant interaction was observed between CYP17A1 and FDX1L, further highlighting the steroidogenic focus. This functional specialization was corroborated by metabolic pathway

analysis, which showed that pre-theca cells contain 12 pathways that were specifically enriched in pre-theca cells relative to other cell types within the ovary. These included fatty acid metabolism, glycerolipid metabolism, pathways in steroid biosynthesis and steroid hormone synthesis pathways (Fig. 6C).

In addition to their metabolic activity, we investigated if pre-theca cells actively communicate with their surroundings through intercellular communication. Secreted signaling analysis suggests a dramatic change in communication between the different types of ovarian cells; at E4.5, pre-theca cells communicated very little with other ovarian cells (Fig. 5D). However, by E6.5 and E8.5, there was a well-developed communication network, mostly involving MK signaling (Fig. 5E, F). Within this computationally predicted signaling axis, pre-theca cells were inferred to serve as candidate signal 'senders' and 'influencers,' while germ cells and pre-granulosa cells were predicted as 'receivers' (Fig. 6D). Overall, these findings reveal that pre-theca cells experience a rapid transcriptomic and metabolic remodeling between E4.5 and E6.5 that enables them to acquire steroidogenic functions and to set up a paracrine regulatory network that may be involved in the regulation of the surrounding ovarian microenvironment to promote the establishment and maintenance of the primordial follicle pool.

Table 1: Differentially expressed genes (DEGs) in chicken embryonic pre-theca cells between E4.5 and E6.5: Data represent transcriptomic profiles identified via scRNA-seq. P-Value: raw p-value; Avg_log2FC: average $\log_2$ fold change between E6.5 and E4.5; PCT.1: percentage of cells expressing the gene in the E6.5 group; PCT.2: percentage of cells expressing the gene in the E4.5 group; P_Val_Adj: adjusted p-value calculated using the non-parametric two-sided Wilcoxon rank-sum test; Threshold: direction of expression (Up-regulated or Down-regulated); Adj_P_Sign and Thr_Sign: classification of significance based on the adjusted p-value and fold-change magnitude.

No	Genes	P-Value	Avg_log^{2}FC	PCT.1	PCT.2	P_Val_Adj	Threshold	Adj_P_Sign	Thr_Sign
1	PPM1H	1.84E-83	3.882769	0.731	0.011	5.42E-79	Up	Highly	Up_Highly
2	PLXNA4	1.65E-68	3.066106	0.462	0.001	4.85E-64	Up	Highly	Up_Highly
3	ADARB2	6.96E-56	2.768606	0.346	0	2.04E-51	Up	Highly	Up_Highly
4	ST8SIA1	2.78E-50	2.770359	0.346	0.001	8.16E-46	Up	Highly	Up_Highly
5	KCNIP4	6.41E-41	2.825607	0.385	0.007	1.88E-36	Up	Highly	Up_Highly
6	PCDH9	2.92E-38	2.385177	0.269	0.001	8.58E-34	Up	Highly	Up_Highly
7	DOCK3	1.09E-37	2.251284	0.231	0	3.19E-33	Up	Highly	Up_Highly
8	NEFM	1.09E-37	2.109671	0.231	0	3.19E-33	Up	Highly	Up_Highly
9	DACT1	3.54E-36	2.525533	0.308	0.004	1.04E-31	Up	Highly	Up_Highly
10	ENSGALG00010009269	2.66E-32	2.473815	0.231	0.001	7.82E-28	Up	Highly	Up_Highly
11	CHRNA9	1.20E-31	1.99861	0.192	0	3.52E-27	Up	Highly	Up_Highly
12	THSD7B	1.20E-31	2.194613	0.192	0	3.52E-27	Up	Highly	Up_Highly
13	ENSGALG00010019341	1.20E-31	2.326808	0.192	0	3.52E-27	Up	Highly	Up_Highly
14	ENSGALG00000031360	1.20E-31	3.030104	0.192	0	3.52E-27	Up	Highly	Up_Highly
15	RPL36AL	1.20E-31	3.968631	0.192	0	3.52E-27	Up	Highly	Up_Highly
16	RPS23	1.20E-31	3.732126	0.192	0	3.52E-27	Up	Highly	Up_Highly
17	RPS21	1.20E-31	4.022091	0.192	0	3.52E-27	Up	Highly	Up_Highly
18	FAU	1.20E-31	2.942798	0.192	0	3.52E-27	Up	Highly	Up_Highly
19	RPS27	1.20E-31	4.461479	0.192	0	3.52E-27	Up	Highly	Up_Highly
20	MT-CO1	1.20E-31	4.832824	0.192	0	3.52E-27	Up	Highly	Up_Highly
21	COII	1.20E-31	4.181288	0.192	0	3.52E-27	Up	Highly	Up_Highly
22	RPS19	1.20E-31	3.515843	0.192	0	3.52E-27	Up	Highly	Up_Highly
23	MAP2	3.52E-30	2.306356	0.269	0.004	1.03E-25	Up	Highly	Up_Highly
24	PCDH17	2.18E-26	1.945723	0.192	0.001	6.39E-22	Up	Highly	Up_Highly
25	KCNK3	1.30E-25	1.799224	0.154	0	3.81E-21	Up	Highly	Up_Highly
26	GATA5	1.30E-25	1.757977	0.154	0	3.81E-21	Up	Highly	Up_Highly
27	RPL14	1.30E-25	2.601541	0.154	0	3.81E-21	Up	Highly	Up_Highly
28	ENSGALG00000043329	1.30E-25	3.033827	0.154	0	3.81E-21	Up	Highly	Up_Highly
29	ENSGALG00000051266	1.30E-25	2.042516	0.154	0	3.81E-21	Up	Highly	Up_Highly
30	ENSGALG00000004509	1.30E-25	2.353839	0.154	0	3.81E-21	Up	Highly	Up_Highly
31	RPS25	1.30E-25	3.343219	0.154	0	3.81E-21	Up	Highly	Up_Highly
32	ENSGALG00000021692	1.30E-25	2.781804	0.154	0	3.81E-21	Up	Highly	Up_Highly
33	GNB2L1	1.30E-25	2.25634	0.154	0	3.81E-21	Up	Highly	Up_Highly
34	MT-ND2	1.30E-25	2.475953	0.154	0	3.81E-21	Up	Highly	Up_Highly
35	FUS	1.30E-25	1.818444	0.154	0	3.81E-21	Up	Highly	Up_Highly
36	HOXA4	2.06E-25	2.480452	0.269	0.007	6.06E-21	Up	Highly	Up_Highly
37	PRSS23	1.26E-22	1.971911	0.192	0.003	3.69E-18	Up	Highly	Up_Highly
38	EPHA6	9.18E-21	3.145671	0.308	0.016	2.69E-16	Up	Highly	Up_Highly
39	SLC16A7	1.67E-20	2.412562	0.231	0.007	4.92E-16	Up	Highly	Up_Highly
40	IFT122	8.39E-20	2.074592	0.192	0.004	2.47E-15	Up	Highly	Up_Highly
41	DPP6	8.91E-20	2.962526	0.308	0.017	2.62E-15	Up	Highly	Up_Highly
42	KCNC2	1.27E-19	2.635712	0.5	0.055	3.73E-15	Up	Highly	Up_Highly
43	POPDC2	1.39E-19	1.528732	0.115	0	4.09E-15	Up	Highly	Up_Highly
44	CDH7	1.39E-19	1.390205	0.115	0	4.09E-15	Up	Highly	Up_Highly
45	MBP	1.39E-19	1.518711	0.115	0	4.09E-15	Up	Highly	Up_Highly
46	DLL1	1.39E-19	1.390205	0.115	0	4.09E-15	Up	Highly	Up_Highly
47	ENSGALG00010019850	1.39E-19	1.818175	0.115	0	4.09E-15	Up	Highly	Up_Highly
48	DOK1	1.39E-19	1.528732	0.115	0	4.09E-15	Up	Highly	Up_Highly
49	SORBS2	1.39E-19	1.540743	0.115	0	4.09E-15	Up	Highly	Up_Highly
50	ZNF367	1.39E-19	1.565537	0.115	0	4.09E-15	Up	Highly	Up_Highly
51	ENSGALG00010020354	1.39E-19	1.362334	0.115	0	4.09E-15	Up	Highly	Up_Highly
52	DYNLT5	1.39E-19	1.366021	0.115	0	4.09E-15	Up	Highly	Up_Highly
53	SPINK5	1.39E-19	1.478015	0.115	0	4.09E-15	Up	Highly	Up_Highly

54	ENSGALG00010028682	1.39E-19	1.528732	0.115	0	4.09E-15	Up	Highly	Up_Highly
55	ENSGALG00010001355	1.39E-19	1.565537	0.115	0	4.09E-15	Up	Highly	Up_Highly
56	ENSGALG00000007131	1.39E-19	1.607978	0.115	0	4.09E-15	Up	Highly	Up_Highly
57	LRP1B	1.39E-19	2.02459	0.115	0	4.09E-15	Up	Highly	Up_Highly
58	EIF3F	1.39E-19	1.558894	0.115	0	4.09E-15	Up	Highly	Up_Highly
59	ENSGALG00000053991	1.39E-19	1.553054	0.115	0	4.09E-15	Up	Highly	Up_Highly
60	ENSGALG00000028749	1.39E-19	1.797771	0.115	0	4.09E-15	Up	Highly	Up_Highly
61	ENSGALG00000006899	1.39E-19	2.00603	0.115	0	4.09E-15	Up	Highly	Up_Highly
62	NDUFB7	1.39E-19	1.501565	0.115	0	4.09E-15	Up	Highly	Up_Highly
63	ENSGALG00000029330	1.39E-19	1.584032	0.115	0	4.09E-15	Up	Highly	Up_Highly
64	LRIG3	4.98E-19	2.459314	0.269	0.013	1.46E-14	Up	Highly	Up_Highly
65	CYP17A1	7.50E-18	-7.28004	0	0.993	2.20E-13	Down	Highly	Down_Highly
66	SYT1	9.06E-18	3.228338	0.346	0.027	2.66E-13	Up	Highly	Up_Highly
67	TNC	1.33E-17	2.087775	0.192	0.006	3.90E-13	Up	Highly	Up_Highly
68	SFRP2	4.13E-15	2.880174	0.308	0.025	1.21E-10	Up	Highly	Up_Highly
69	PBX3	5.67E-15	2.598747	0.346	0.034	1.67E-10	Up	Highly	Up_Highly
70	ENSGALG00010015186	6.40E-15	3.742318	0.615	0.128	1.88E-10	Up	Highly	Up_Highly
71	TSHZ1	8.46E-15	1.383862	0.115	0.001	2.49E-10	Up	Highly	Up_Highly
72	S100A10	8.46E-15	2.25029	0.115	0.001	2.49E-10	Up	Highly	Up_Highly
73	HOXA3	9.94E-15	2.112972	0.154	0.004	2.92E-10	Up	Highly	Up_Highly
74	SMAD6	2.10E-14	2.181455	0.308	0.027	6.16E-10	Up	Highly	Up_Highly
75	ADAMTSL3	2.62E-14	2.624777	0.269	0.02	7.71E-10	Up	Highly	Up_Highly
76	ZFAND1	3.37E-14	2.120361	0.269	0.02	9.91E-10	Up	Highly	Up_Highly
77	VIM	9.57E-14	3.01092	0.769	0.274	2.81E-09	Up	Highly	Up_Highly
78	LPIN2	2.68E-13	2.072491	0.308	0.03	7.86E-09	Up	Highly	Up_Highly
79	SFRP1	2.98E-13	2.532537	0.346	0.039	8.75E-09	Up	Highly	Up_Highly
80	FAM171A1	3.25E-13	2.087573	0.231	0.016	9.55E-09	Up	Highly	Up_Highly
81	CSRP2	6.60E-13	1.751133	0.154	0.006	1.94E-08	Up	Highly	Up_Highly
82	TENM1	6.60E-13	3.027423	0.154	0.006	1.94E-08	Up	Highly	Up_Highly
83	KCNAB1	3.57E-12	2.019713	0.192	0.011	1.05E-07	Up	Highly	Up_Highly
84	CACNA1C	5.38E-12	2.636752	0.731	0.271	1.58E-07	Up	Highly	Up_Highly
85	MTUS1	6.42E-12	1.552279	0.115	0.003	1.89E-07	Up	Highly	Up_Highly
86	ORC2	6.42E-12	1.552945	0.115	0.003	1.89E-07	Up	Highly	Up_Highly
87	RFT1	7.05E-12	1.347917	0.115	0.003	2.07E-07	Up	Highly	Up_Highly
88	ERCC6L2	8.47E-12	1.457019	0.115	0.003	2.49E-07	Up	Highly	Up_Highly
89	TXN	1.72E-11	-2.44995	0.308	0.942	5.05E-07	Down	Highly	Down_Highly
90	ENSGALG00010019818	1.74E-11	1.675081	0.154	0.007	5.10E-07	Up	Highly	Up_Highly
91	CEP63	1.74E-11	1.623105	0.154	0.007	5.10E-07	Up	Highly	Up_Highly
92	TENM2	5.40E-11	2.273581	0.269	0.028	1.59E-06	Up	Highly	Up_Highly
93	NR2F1	3.59E-10	2.209484	0.269	0.031	1.05E-05	Up	Highly	Up_Highly
94	COBL	5.43E-10	1.749058	0.115	0.004	1.59E-05	Up	Highly	Up_Highly
95	FAM214B	5.43E-10	1.311902	0.115	0.004	1.59E-05	Up	Highly	Up_Highly
96	ID2	7.59E-10	2.780508	0.308	0.044	2.23E-05	Up	Highly	Up_Highly
97	PI4K2B	9.02E-10	1.706108	0.192	0.016	2.65E-05	Up	Highly	Up_Highly
98	SMIM3	1.23E-09	1.900398	0.231	0.024	3.63E-05	Up	Highly	Up_Highly
99	USMG5	1.44E-09	2.186796	0.692	0.298	4.23E-05	Up	Highly	Up_Highly
100	HCFC2	2.04E-09	1.594382	0.154	0.01	5.99E-05	Up	Highly	Up_Highly
101	PTS	2.75E-09	1.933152	0.231	0.025	8.09E-05	Up	Highly	Up_Highly
102	RPS26	3.76E-09	1.058155	1	0.88	0.000111	Up	Highly	Up_Highly
103	ECHDC2	9.20E-09	1.927446	0.192	0.018	0.00027	Up	Highly	Up_Highly
104	NFAT5	1.11E-08	1.774703	0.192	0.018	0.000326	Up	Highly	Up_Highly
105	HDAC10	1.23E-08	1.6096	0.154	0.011	0.00036	Up	Highly	Up_Highly
106	ACAD11	1.23E-08	1.677007	0.154	0.011	0.00036	Up	Highly	Up_Highly
107	HAND2	1.30E-08	1.343105	0.115	0.006	0.000383	Up	Highly	Up_Highly
108	XRN1	1.30E-08	1.439867	0.115	0.006	0.000383	Up	Highly	Up_Highly
109	H6PD	1.30E-08	1.388361	0.115	0.006	0.000383	Up	Highly	Up_Highly
110	VPS13C	1.39E-08	1.407999	0.115	0.006	0.000409	Up	Highly	Up_Highly
111	GPAT3	1.44E-08	1.310864	0.115	0.006	0.000423	Up	Highly	Up_Highly
112	CHRM3	1.63E-08	1.536838	0.154	0.011	0.00048	Up	Highly	Up_Highly
113	ENSGALG00010015519	2.06E-08	2.79684	0.346	0.068	0.000604	Up	Highly	Up_Highly
114	SPON1	2.09E-08	-3.47882	0	0.626	0.000613	Down	Highly	Down_Highly
115	EXOSC3	2.70E-08	1.858027	0.192	0.02	0.000794	Up	Highly	Up_Highly
116	SDHAF4	2.90E-08	1.929468	0.308	0.052	0.000851	Up	Highly	Up_Highly
117	CSMD1	4.94E-08	1.600748	0.192	0.02	0.001451	Up	Highly	Up_Highly
118	HAUS6	5.60E-08	1.796583	0.154	0.013	0.001645	Up	Highly	Up_Highly
119	NES	6.14E-08	1.525701	0.154	0.013	0.001804	Up	Highly	Up_Highly
120	MTPAP	6.43E-08	1.968005	0.231	0.031	0.001889	Up	Highly	Up_Highly
121	ENSGALG00010002666	6.70E-08	2.592284	0.269	0.042	0.001969	Up	Highly	Up_Highly
122	HMGCL	9.08E-08	1.885125	0.346	0.071	0.002666	Up	Highly	Up_Highly
123	BMP5	1.43E-07	1.997811	0.115	0.007	0.004191	Up	Highly	Up_Highly
124	SFXN2	1.43E-07	1.332909	0.115	0.007	0.004191	Up	Highly	Up_Highly
125	TBCCD1	1.43E-07	1.43043	0.115	0.007	0.004191	Up	Highly	Up_Highly
126	MTMR1	1.75E-07	1.873526	0.192	0.023	0.00515	Up	Lowly	Up_Lowly
127	BASP1	2.26E-07	-1.66475	0.308	0.856	0.006631	Down	Lowly	Down_Lowly
128	GHITM	2.39E-07	1.917232	0.462	0.142	0.007009	Up	Lowly	Up_Lowly
129	APOA1	3.08E-07	-3.30087	0	0.561	0.00905	Down	Lowly	Down_Lowly

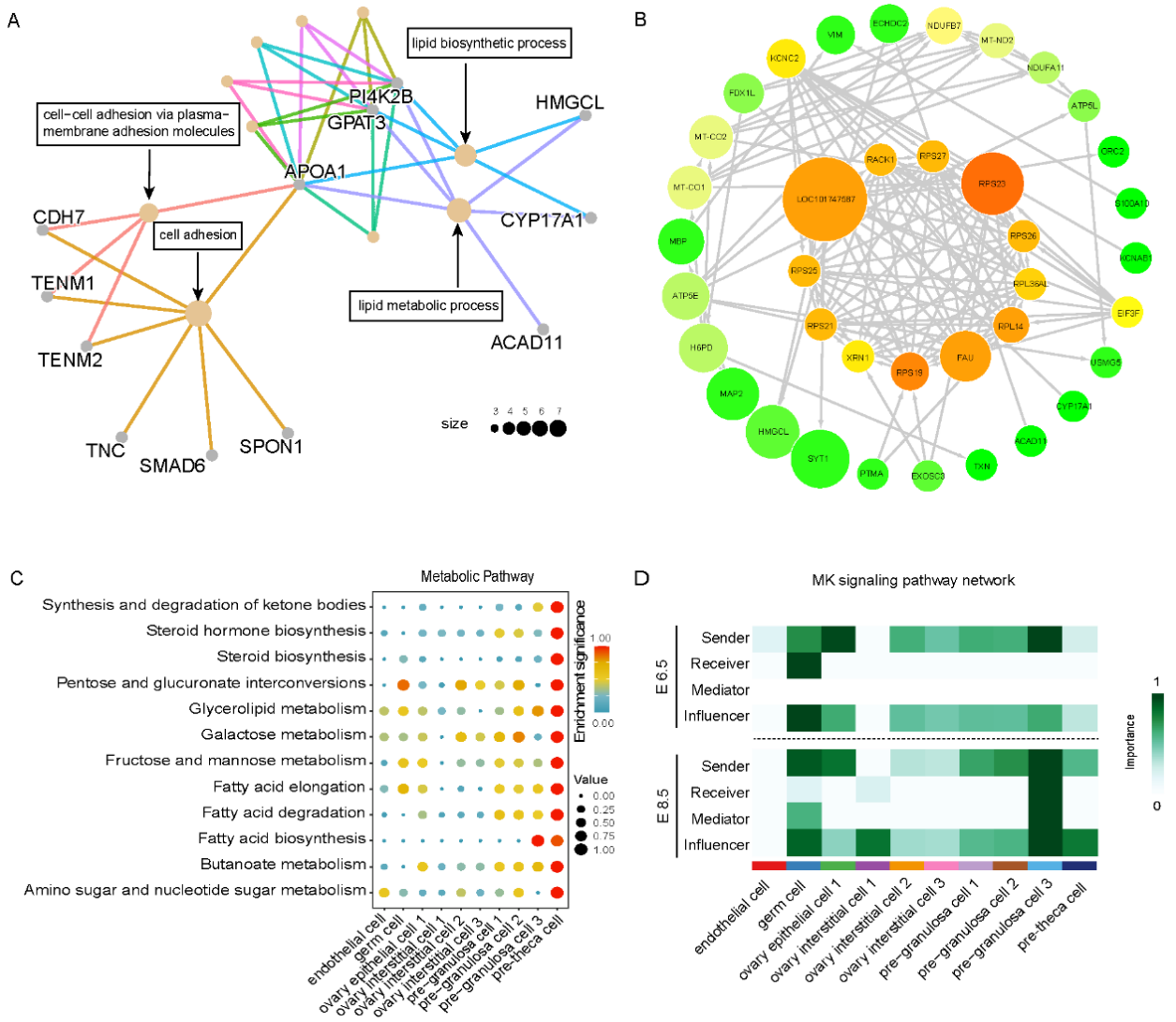


Fig. 6: Metabolic and signaling networks supporting the steroidogenic function of pre-theca cells: (A) Cnet plot of Gene Ontology (GO) enrichment for DEGs between E4.5 and E6.5. (B) Protein-protein interaction (PPI) network of core differentially expressed proteins; node size and color indicate degree and betweenness centrality, respectively. (C) Dot plot of specifically enriched metabolic pathways in pre-theca cells. (D) Heatmap of the MK signaling pathway network, highlighting the roles of pre-theca cells as signal senders/influencers and germ/pre-granulosa cells as receivers.

DISCUSSION

Theca cells in the embryonic gonads of females of avians have not been extensively investigated till date. In this study, the single-cell RNA sequencing (scRNA-seq) analysis of chicken embryonic gonads revealed population of pre-theca cells suggesting their early emergence in the process of gonadal development as early as embryonic day 4.5 (E4.5). The present finding was corroborated by pre-theca cells which have been identified by fluorescence in situ hybridization (FISH) with a probe for *CYP11A1*, which suggest that cells of the pre-theca differentiate before the morphological development of primordial follicles. Such early differentiation is an important event since the assembly of primordial follicles forms the ovarian reserve and the reproductive lifespan and productivity of the hen will depend on the number of follicles in the ovarian reserve. The FISH analysis used a single probe (CYP11A1); dual-marker in situ detection will be needed to define the identity of these cells conclusively.

These findings are in agreement with previous reports of expression of *CYP11A1* in the gonads of the female chicken embryo (Carré *et al.*, 2011; Estermann *et al.*, 2020). In contrast, the pre-theca cells seem to be absent in human embryonic gonads and post-neonatal mouse ovary until the appearance of secondary follicles (Liu *et al.*, 2020). This timing and mechanism of pre-theca cell differentiation have been found to be different between avian and mammalian species.

These differences in the timing of pre-theca cell differentiation may be a result of different developmental constraints. As, chicken development depends on the nutrients which are limited within the egg, while mammalian development depends on continuous maternal circulation through the placenta (Givisiez *et al.*, 2020). Pre-theca cells in the chicken ovary were identified prior to the onset of primordial follicle formation and found to express the well-established markers of pre-theca cells, *CYP11A1*, *CYP17A1*, *STAR*, *NR5A1* and *HSD3B1*. In our previous studies, it was shown that the pharmacological inhibition of steroid hormone synthesis in pre-theca cells, totally blocked the formation of primordial follicles (Yu *et al.*, 2024). In avian reproductive biology and theriogenology, the establishment of the primordial follicle pool defines the

biological foundation of the ovarian reserve. While our spatiotemporal multi-omics and histological data demonstrate that pre-theca cells differentiate prior to primordial follicle assembly, these observations reflect a strong spatial and endocrine association rather than cell-autonomous causality. In mammalian models, definitive functional proof relies on targeted cell-ablation tools (such as inducible Cre-loxP or diphtheria toxin systems), which are currently unavailable for avian theca lineages. Nonetheless, the functional requirement of the steroidogenic microenvironment supplied by these early somatic cells is supported by our prior in vivo pharmacological work, where systemic inhibition of cholesterol and estrogen synthesis (via simvastatin and tamoxifen) completely arrested primordial follicle formation at 5.5 dph (Yu *et al.*, 2024). Future advances in avian transgenesis will be valuable to achieve cell-specific genetic ablation and definitively isolate the autonomous regulatory roles of pre-theca cells. This indicates that the pre-theca cells are the main steroidogenic component that is necessary to trigger the assembly of the ovarian reserve. In contrast, in human embryonic or neonatal mouse ovaries these are not expressed until the antral follicle stage. These marker genes encode key enzymes in the steroid hormone synthesis pathway: *CYP11A1* catalyzes the first step to convert cholesterol to pregnenolone, while *CYP17A1* is required for biosynthesis of the following steroid hormones (Guo *et al.*, 2007; Porubek, 2013). Moreover, NR5A1 (steroidogenic factor 1) is a critical transcription factor in gonadal development and *HSD3B1* is an important enzyme of the androgen metabolism pathway (Bashamboo and McElreavey, 2010; Hettel *et al.*, 2018). Interestingly, expressions of *CYP17A1* and *HSD17B3* is observed in the placenta, not in embryonic gonads, which is unlike the expression of *CYP11A1* and *CYP19A1* as seen in avians (Dickson *et al.*, 2023; Yazawa *et al.*, 2023). Collectively, these results suggest that the steroid hormone synthesis pathway is activated earlier in the development of the avian gonads compared to mammals.

Moreover, this study provides the first description of the developmental trajectory of pre-theca cells using single-cell sequencing. We found three subpopulations which mature in a continuous linear pattern. Along this trajectory, there was a gradual increase in the expression of the genes of *CYP17A1*, *CYP11A1*, *STAR*, and *HSD3B1*, which was also observed in the gonads of female chicken embryos (Carré *et al.*, 2011), furthermore, it revealed significant upregulation of *CYP17A1*, *LHCGR*, *CYP11A1*, *HSD3B1* and *SMAD7* in late-stage gonads. We note that pseudotime trajectories inferred by Monocle3 and CytoTRACE reflect in silico models based on transcriptional dynamics rather than direct in vivo lineage tracing. While the continuous upregulation of steroidogenic along this axis is biologically concordant with functional maturation, experimental lineage-tracing tools will be required to definitively confirm this developmental progression in avian gonads. Therefore, our findings give an intuitive spatial and temporal map of the maturation of pre-theca cells. The analysis of the embryonic gonadal proteomic data also suggested that typical pre-theca markers (*CYP11A1*, *CYP17A1*, *NR5A1* and *STAR*) were expressed at significantly higher levels in female gonads compared to male gonads and were differentially expressed by sex-reversal treatment. These markers have also been demonstrated in other species, such as medaka fish, in which the Cyp17a1 gene is knocked out and leads to a complete all-male sex phenotype with testis-like gonads that produce fertile sperm, and in Nile tilapia, in which the Cyp17a1 gene is knocked out and results in an all-male sex phenotype with testis-like gonads that produce fertile sperm (Sato *et al.*, 2008; Yang *et al.*, 2021). A *CYP17A1* knockout chicken model has not been developed yet, other species like *Pogona vitticeps* indicate that *NR5A1* is a potential sex determination candidate, as a partially truncated product of NR5A1 protein in the ZW chicken may competitively interfere with functional *NR5A1* to drive female development (Zhang *et al.*, 2022). These observations, it is believed that the pre-theca cells may be important in the sex determination process in chicken although there is still much to be understood concerning the regulatory mechanisms.

In addition, we found 129 DEGs in the pre-theca cells between E4.5 and E6.5, with significant enrichment in cell adhesion, lipid metabolism and lipid biosynthesis. The higher abundance of lipid biosynthesis pathways in pre-theca cells implies that steroid hormone production and its ability to build up the ovarian reserve is tightly coupled to metabolic availability. In teleost fish, starvation-induced changes in lipid metabolism have been found to lead to sex reversal from female to male in medaka (Sakae *et al.*, 2020). Likewise, pathways of lipid metabolism have been linked to chicken germ cell differentiation (Zuo *et al.*, 2015). Our analysis identified 12 metabolic pathways are specifically enriched in pre-theca cells such as fatty acid biosynthesis, glycerolipid biosynthesis and steroid hormone biosynthesis. Therefore, pre-theca cells likely contribute to embryonic development and sex differentiation through the coordination of lipid and steroid metabolic pathways. Additionally, while CellChat prioritized midkine (MK) signaling as a primary channel between pre-theca and neighboring germ/pre-granulosa cells, these ligand–receptor predictions reflect mRNA co-expression rather than direct biochemical signaling; experimental validation will be necessary to confirm functional activation of these candidate paracrine pathways. Our in vivo pharmacological evidence, where blocking cholesterol substrate availability (via simvastatin) or estrogen receptor signaling (via tamoxifen) completely arrested primordial follicle formation at 5.5 dph (Yu *et al.*, 2024). Future studies using ultra-sensitive micro-scale LC-MS/MS will be valuable to quantify the exact steroid flux during these embryonic stages.

Conclusions: In conclusion pre-theca cells make their differentiation before the emergence of primordial follicles and establish the molecular foundation for the ovarian reserve significantly earlier than in mice or humans. We have elucidated a linear developmental pathway in which the steroidogenic potential is gradually acquired, and found specific markers such as *CYP17A1*, *TXN*, *SPON1*, *BASP1* and *APOA1* that define the transition to a mature metabolic state. The primordial follicle pool is assembled in the presence of lipid metabolism and steroid hormone synthesis by pre-theca cells. These findings provide a basis for future functional studies on ovarian development and reproductive biology in poultry. Understanding the

regulatory mechanisms of pre-theca cells provides a new perspective to improve avian reproductive health and offers potential targets for optimizing the reproductive productivity of poultry.

Ethics statement: All animal experiments were conducted in strict accordance with the Guidelines for the Care and Use of Laboratory Animals and were approved by the Animal Experiments Ethics Committee of Ganzhou Polytechnic, NO. S20260811.

Author's contributions: LY, ARJ conceived and designed the study; LY executed the experiments; LY, ARJ collected and processed the data; LY, ARJ interpreted the data; LY, ARJ, XX, LY, MHA collaborated on drafting and revising the manuscript; LY, ARJ provided technical guidance, supervision, and secured funding support; All authors interpreted the data, critically revised the manuscript for important intellectual contents, and approved the final version.

Funding: This work was supported by the Science and Technology Research Project of Ganzhou Polytechnic (Grant No. X-2025-KXJS-03).

Acknowledgement: The authors extend their appreciations to the Ongoing Research Funding Program, (ORF-2026-191), King Saud University, Riyadh, Saudi Arabia

REFERENCES

Ayers KL, Lambeth LS, Davidson NM, *et al.*, 2015. Identification of candidate gonadal sex differentiation genes in the chicken embryo using RNA-seq. BMC Genomics 16:704.

Bashamboo A and Mcelreavey K, 2010. NR5A1/SF-1 and development and function of the ovary. Annales d'Endocrinologie 71:177-182.

Carré G-A, Couty I, Hennequet-Antier C, *et al.*, 2011. Gene expression profiling reveals new potential players of gonad differentiation in the chicken embryo. PLoS One 6:e23959.

Dickson A, Yutuc E, Thornton CA, *et al.*, 2023. HSD3B1 is an oxysterol 3β-hydroxysteroid dehydrogenase in human placenta. Open Biology 13:220313.

Edson MA, Nagaraja AK and Matzuk MM, 2009. The mammalian ovary from genesis to revelation. Endocrine Reviews 30:624-712.

Erickson GF, Magoffin DA, Dyer CA, *et al.*, 1985. The ovarian androgen producing cells: a review of structure/function relationships. Endocrine Reviews 6:371-399.

Estermann MA, Williams S, Hirst CE, *et al.*, 2020. Insights into gonadal sex differentiation provided by single-cell transcriptomics in the chicken embryo. Cell Reports 31:107491.

Ford EA, Beckett EL, Roman SD, *et al.*, 2020. Advances in human primordial follicle activation and premature ovarian insufficiency. Reproduction 159:R15-r29.

Givisiez PEN, Moreira Filho ALB, Santos MRB, *et al.*, 2020. Chicken embryo development: metabolic and morphological basis for in ovo feeding technology. Poultry Science 99:6774-6782.

Guo IC, Shih MC, Lan HC, *et al.*, 2007. Transcriptional regulation of human CYP11A1 in gonads and adrenals. Journal of Biomedical Science 14:509-15.

Hettel D, Zhang A, Alyamani M, *et al.*, 2018. AR signaling in prostate cancer regulates a feed-forward mechanism of androgen synthesis by way of HSD3B1 upregulation. Endocrinology 159:2884-2890.

Hirshfield AN, 1991. Theca cells may be present at the outset of follicular growth. Biology of Reproduction 44:1157-1162.

Jung KM, Seo M, Kim YM, *et al.*, 2021. Single-cell RNA sequencing revealed the heterogeneity of gonadal primordial germ cells in zebra finch (Taeniopygia guttata). Frontiers in Cell and Developmental Biology 9:791335.

Kerr JB, Duckett R, Myers M, *et al.*, 2006. Quantification of healthy follicles in the neonatal and adult mouse ovary: evidence for maintenance of primordial follicle supply. Reproduction 132:95-109.

Lavoie HA and King SR, 2009. Transcriptional regulation of steroidogenic genes: STARD1, CYP11A1 and HSD3B. Experimental Biology and Medicine 234:880-907.

Lenz S, Pöhland R, Becker F, *et al.*, 2004. Expression of the bovine aromatase cytochrome P450 gene (Cyp19) is primarily regulated by promoter 2 in bovine follicles and by promoter 1.1 in corpora lutea. Molecular Reproduction and Development: Incorporating Gamete Research 67:406-413.

Li Y, Gao D, Xu T, *et al.*, 2020. Anti-Müllerian hormone inhibits luteinizing hormone-induced androstenedione synthesis in porcine theca cells. Theriogenology 142:421-432.

Liu T, Qin Q-Y, Qu J-X, *et al.*, 2020. Where are the theca cells from: the mechanism of theca cells derivation and differentiation. Chinese Medical Journal 133:1711-1718.

Lo BK, Sheikh S and Williams Sa SA, 2019. In vitro and in vivo mouse follicle development in ovaries and reaggregated ovaries. Reproduction 157:135-148.

Lu J, Zhang X, Wang Q, *et al.*, 2024. Effects of exogenous energy on synthesis of steroid hormones and expression characteristics of the CREB/StAR signaling pathway in theca cells of laying hen. Poultry Science 103:103414.

Mourikes VE, Santacruz Márquez R, Deviney A, *et al.*, 2023. Imidacloprid and its bioactive metabolite, desnitro-imidacloprid, differentially affect ovarian antral follicle growth, morphology, and hormone synthesis in vitro. Toxics 11:349.

Nakata T, Ishiguro M, Aduma N, *et al.*, 2013. Chicken hemogen homolog is involved in the chicken-specific sex-determining mechanism. Proceedings of the National Academy of Sciences 110:3417-3422.

Porubek D, 2013. CYP17A1: a biochemistry, chemistry, and clinical review. Current Topics in Medicinal Chemistry 13:1364-84.

Sakae Y, Oikawa A, Sugiura Y, *et al.*, 2020. Starvation causes female-to-male sex reversal through lipid metabolism in the teleost fish, medaka (Oryzias latipes). Biology Open 9:bio050054.

Sato T, Suzuki A, Shibata N, *et al.*, 2008. The novel mutant scl of the medaka fish, Oryzias latipes, shows no secondary sex characters. Zoological Science 25:299-306.

Schwartz JR and Roy SK, 2000. Developmental expression of cytochrome P450 side-chain cleavage and cytochrome P450 17α-hydroxylase messenger ribonucleic acid and protein in the neonatal hamster ovary. Biology of Reproduction 63:1586-1593.

Smith CA and Sinclair AH, 2004. Sex determination: insights from the chicken. Bioessays 26:120-132.

Yang L, Zhang X, Liu S, *et al.*, 2021. Cyp17a1 is required for female sex determination and male fertility by regulating sex steroid biosynthesis in fish. Endocrinology 162:bqab205.

Yang Y, Li X, Ye S, *et al.*, 2022. Identification of genes related to sexual differentiation and sterility in embryonic gonads of Mule ducks by transcriptome analysis. Frontiers in Genetics 13:1037810.

Yazawa T, Islam MS, Imamichi Y, *et al.*, 2023. Comparison of Placental HSD17B1 Expression and Its Regulation in Various Mammalian Species. Animals (Basel) 13:622.

Yu L, Peng R, Liang J, *et al.*, 2024. Spatiotemporal single-cell RNA sequencing reveals the role of steroid hormone pathway during chicken primordial follicle formation. Poultry Science 103:104090.

Yuan C, Chen X, Shen C, *et al.*, 2022. Follicular fluid exosomes regulate oxidative stress resistance, proliferation, and steroid synthesis in porcine theca cells. Theriogenology 194:75-82.

Zhang X, Wagner S, Holleley CE, *et al.*, 2022. Sex-specific splicing of Z- and W-borne nr5a1 alleles suggests sex determination is controlled by chromosome conformation. Proceedings of the National Academy of Sciences of the United States of America 119:e2116475119.

Zuo Q, Li D, Zhang L, *et al.*, 2015. Study on the regulatory mechanism of the lipid metabolism pathways during chicken male germ cell differentiation based on RNA-seq. PLoS One 10:e0109469.